



Activation of miR-21 by STAT3 Induces Proliferation and Suppresses Apoptosis in Nasopharyngeal Carcinoma by Targeting PTEN Gene

Hesheng Ou¹, Yumei Li¹, Min Kang^{2*}

1 College of Pharmacy, Guangxi Medical University, Nanning City, Guangxi Province, P.R. China, **2** The First Affiliated Hospital, Guangxi Medical University, Nanning City, Guangxi Province, P.R. China

Abstract

The present study is to investigate the role of microRNA-21 (miR-21) in nasopharyngeal carcinoma (NPC) and the mechanisms of regulation of PTEN by miR-21. Fifty-four tissue samples were collected from 42 patients with NPC and 12 healthy controls. Human NPC cell lines CNE-1, CNE-2, TWO3 and C666-1 were used for cell assays. To investigate the expression of miR-21, RT-PCR was employed. RT-PCR, Western blotting, and immunohistochemistry were used to measure the expression of STAT3 mRNA and STAT3 protein. To test the effect of miR-21 on the cell growth and apoptosis of NPC cells *in vitro*, transfection of CNE1 and CNE2 cell lines and flow cytometry were performed. TUNEL assay was used to detect DNA fragmentation. To validate whether miR-21 directly recognizes the 3'-UTRs of PTEN mRNA, luciferase reporter assay was employed. miR-21 expression was increased in NPC tissues compared with control and the same result was found in NPC cell lines. Notably, increased expression of miR-21 was directly related to advanced clinical stage and lymph node metastasis. STAT3, a transcription factor activated by IL-6, directly activated miR-21 in transformed NPC cell lines. Furthermore, miR-21 markedly inhibited PTEN tumor suppressor, leading to increased AKT activity. Both *in vitro* and *in vivo* assays revealed that miR-21 enhanced NPC cell proliferation and suppressed apoptosis. miR-21, activated by STAT3, induced proliferation and suppressed apoptosis in NPC by targeting PTEN-AKT pathway.

Citation: Ou H, Li Y, Kang M (2014) Activation of miR-21 by STAT3 Induces Proliferation and Suppresses Apoptosis in Nasopharyngeal Carcinoma by Targeting PTEN Gene. PLoS ONE 9(11): e109929. doi:10.1371/journal.pone.0109929

Editor: Jin Q. Cheng, H. Lee Moffitt Cancer Center & Research Institute, United States of America

Received: May 14, 2014; **Accepted:** September 12, 2014; **Published:** November 3, 2014

Copyright: © 2014 Ou et al. This is an open-access article distributed under the terms of the Creative Commons Attribution License, which permits unrestricted use, distribution, and reproduction in any medium, provided the original author and source are credited.

Data Availability: The authors confirm that all data underlying the findings are fully available without restriction. All relevant data are within the paper.

Funding: This study was supported by grants from the National Natural Science Foundation of China (No. 81373403, Hesheng Ou), Research Foundation of the Education Department of Guangxi Province, China (No. 2013YB049, Hesheng Ou), Research Foundation from the Regional Health Department of Guangxi Province, China (No. Z2012066, Min Kang), and Youth Foundation of Guangxi Medical University, China (No. 02604001020, Min Kang). The funders had no role in study design, data collection and analysis, decision to publish, or preparation of the manuscript.

Competing Interests: The authors have declared that no competing interests exist.

* Email: km10192013@126.com

Introduction

Nasopharyngeal carcinoma (NPC) causes 80,000 new cases and 50,000 deaths every year [1], [2]. NPC is mainly a non-lymphomatous, non-keratinizing, squamous cell carcinoma, which is highly malignant with abilities of local invasion and early distant metastasis [1]. Genetic susceptibility, endemic environment factors, and Epstein-Barr virus infection are believed to be the major etiologic factors of NPC [3–5]. Currently, the standard care for these patients consists of concurrent chemoradiotherapy with cisplatin-based regimens, generally followed by adjuvant chemotherapy. The 5-year survival rate for patients with NPC remains about 70%. However, systemic and local side effects caused by chemotherapy greatly tormented the patients physically and psychologically. Therefore, it is of importance to study the precise molecular mechanisms of NPC and explore new, safe and effective NPC therapies.

MicroRNAs (miRNAs) are small non-coding RNAs (20 to 24 nucleotides) that post-transcriptionally modulate gene expression by negatively regulating the stability or translational efficiency of their target mRNAs [6]. Increasing data showed that miRNAs played an important role in cancer, and a concept of “oncomirs”

was proposed [7]. Among them, miR-21 emerged as a key oncomir, since it was consistently up-regulated in a wide range of cancers [8–11], and implicated in multiple malignancy-related processes such as cell proliferation, apoptosis, invasion, and metastasis [12–15]. Functional studies showed that knockdown of miR-21 led to reduced proliferation and tumor growth in MCF-7 cells [16], [17], and reduced invasion and metastasis in MDA-MB-231 cells [17]. These data clearly implicated that miR-21 acted as a key molecule in carcinogenesis. However, the mechanisms by which miR-21 acts in the development of NPC still remain unknown, and no miR-21 targets were reported in NPC.

Persistent activation of signal transducer and activator of transcription (STAT) has been observed and is frequently associated with malignant transformation [18]. Constitutive activation of STAT proteins, notably of STAT3, is detected in many human tumor cells and cells transformed by oncoproteins [19–21]. STAT3 is a well-characterized transcription factor that has been demonstrated to contribute to various processes of tumorigenesis, such as tumor cell survival and proliferation, invasion, angiogenesis and drug resistance [22]. Aberrant STAT3 enhances uncontrolled growth and survival of cancer cells through

dysregulation of gene expression, including cyclin D1 [23], c-Myc [24], and survivin genes [25], and hence, contributing to tumorigenesis.

The enzyme phosphatase and tensin homologue (PTEN) gene is one of the most frequently inactivated tumor suppressor genes in a variety of cancers. Inactivating mutations and deletions of the PTEN gene are found in many types of cancers, including NPC [26]. It is reported that PTEN gene inhibits Akt activation (phosphorylation) [27–28], which plays a central role in an outermost complex network of cell growth modulation that affects protein biosynthesis, cell cycle arrest and apoptosis [29], [30]. Interestingly, 3'-UTR of PTEN gene has been proved to harbor a putative binding site for miR-21 by bioinformatics tools. Therefore, we hypothesize that PTEN gene is regulated by miR-21 as one of the several miR-21 target genes in NPC. The present study is to investigate the role of miR-21 in NPC and the mechanisms of regulation of PTEN by miR-21.

Materials and Methods

Patients and tissue samples

Fifty-four tissue samples were collected from 42 patients with NPC and 12 healthy controls. The 42 NPC patients comprised 22 early cases and 22 advanced cases, whose clinical and pathological data were displayed in Table 1. Tissue samples were immediately frozen in liquid nitrogen after resection and stored at -80°C until use. Both tumor and non-tumor samples were confirmed by the pathological examinations. The clinical stage was defined according to the 2002 AJCC/UICC staging classifications. The pathological stage, grade, and nodal status were appraised by an experienced pathologist. Clinicopathologic characteristics including gender, age, pathology, differentiation, and tumor-node-metastasis staging have been collected.

Written informed consent was obtained from all participants. Collections and using of tissue samples were approved by the The

Human Research Ethics Committee of The First Affiliated Hospital of Guangxi Medical University. The procedures are in accordance with the Helsinki Declaration of 1975.

Cell culture, transfection and establishment of stable cell lines

Human NPC cell lines CNE-1, CNE-2, TWO3 and C666-1 were purchased from Cell Application (Santiago, USA) and were cultured in Dulbecco's Modified Eagle Medium containing 10% fetal bovine serum, 100 IU/ml penicillin and 100 $\mu\text{g}/\text{ml}$ streptomycin in humidified 5% CO_2 atmosphere at 37°C as previously described [31]. Primary cells between passage 4 and 10 were used in the experiments and in the establishment of stable cell lines. For transfection, cells were grown up to 90% confluency, and were transfected with small interfering RNA (siRNA) or miRNA plasmids using Lipofectamine 2000 (Life Technologies, USA) by incubating with OptiMem-I media for 4 h. The cells were then transferred into fresh Dulbecco's Modified Eagle Medium with 10% fetal bovine serum. To establish stable cell lines with miRNA overexpression, G418 (1 mg/ml; Invitrogen, USA) was added into the medium 2 days after transfection with selective medium being changed once a week. The transfected cells expressing neomycin-resistant gene survived in the selective medium with the elimination of the non-transfected cells. The cells were individually picked 2 weeks later using conventional cloning techniques for expansion. Passages 2–10 of the stable cell lines were identified by verifying miRNA expression with Northern blotting and *in situ* hybridization as previously described [32], and were used for experiments.

Immunohistochemistry

The selected tumor tissues were used to construct tissue microarray slides. Paraffin sections were cut and mounted on glass slides, and 5 μm sections from formalin-fixed and paraffin-embedded specimens were deparaffinized using xylene and

Table 1. Clinicopathologic characteristics of NPC patients aged between 30 and 74, with a median age of 48.

Characteristics		Number of patients (%)
Gender	Male	31/42 (73.8)
	Female	11/42 (26.2)
Age (years)	<60	30/42 (71.4)
	≥ 60	12/42 (28.6)
TNM stage	I+II	20/42 (47.6)
	III+IV	22/42 (52.4)
Lymph node metastasis	Positive	24/42 (57.1)
	Negative	18/42 (42.9)
Distant metastasis	Positive	5/42 (11.9)
	Negative	37/42 (88.1)
Pathologic type	WHO II	4/42 (9.5)
	WHO III	38/42 (90.5)
Smoking and alcohol consumption history	Smoking	30/42 (71.4)
	Non-smoking	12/42 (28.6)
	Alcoholic	26/42 (61.9)
	Non-alcoholic	16/42 (38.1)

Note: Primary tumors at pharynx nasalis in NPC had deep, wide and irregular invasions into peripheral tissues, so the sizes of these tumors could not be measured in the evaluation of NPC staging. None of the NPC patients received any treatment before. Before standard chemotherapies or radiotherapies, tissue biopsies from pharynx nasalis were examined. For subsequent treatment for NPC, concurrent chemoradiotherapy plus adjuvant chemotherapy were performed.

doi:10.1371/journal.pone.0109929.t001

rehydrated in graded ethanol. Samples were then preincubated with 3% H₂O₂ to eliminate endogenous peroxidase activity. Antigen retrieval was achieved by heating the sections for 2 min at 100°C in citric acid buffer (0.01 mol/L, pH 6.0). Immunohistochemistry was performed by the two-step method using primary antibody, including heat-induced antigen-retrieval procedures. Sections were incubated overnight at 37°C with primary antibody. After the primary antibody was washed off, the components of the EnVision Detection System were applied with an anti-mouse polymer (EnVision1/HRP/Mo, Dako, Glostrup, Denmark). The primary antibodies used were all mouse anti-human monoclonal antibodies against STAT3, BCL-2 and BAX (1:100 dilution; American Research Products, Belmont, USA). Negative controls were treated identically but with the primary antibody being omitted.

Immunoreactivity was evaluated independently by three researchers. The percentage of positive tumor cells was determined by each observer, and the average of the 3 scores was calculated. Ten high-power fields were randomly selected and 1,000 cells were counted in each core. When the mean of percentage of positive cells was close to 0% or 100%, the standard deviation (SD) was close to 0. When the mean was approximately 50%, the SD was approximately 5%. Therefore, the SD did not increase with the mean. The following categories were used for scoring: none (0), mild (1), moderate (2), and strong (3) for the intensity of staining; <5% (0), 5–25% (1), 25–50% (2), and >50% (3) for the percentage of positive staining. The combination of the intensity and percentage of staining resulted in the following scores: 0–1, negative (-); 2–4, moderate (+); 5–6 strong (++) [33], [34].

Real-time polymerase chain reaction (RT-PCR) analysis

Total RNA was extracted using Trizol reagent (Invitrogen, USA) for miR-21, STAT3 mRNA and PTEN mRNA analyses. For the detection of miR-21 expression, stem-loop RT-PCR was performed as previously described [35]. Quantitative PCR (qPCR) was carried out using SYBR Premix Ex Taq (Takara, Japan) according to the manufacturer's protocol. Relative expression was evaluated by comparative CT method and normalized to the expression of U6 small RNA. The primers for miR-21 are as follows: stem-loop RT primer, 5'-GTCGTATCCAGTGCAGGGTCCGAGGTATTGCGCACTGGATACGACTCAACA-3'; forward primer, 5'-GCCCGCTAGCTTATCAGACTGATG-3', and reverse primer, 5'-GTGCAGGGTCCGAGGT-3'. The primers for U6 are as follows: RT primer, 5'-GTCGTATCCAGTGCAGGGTCCGAGGTATTGCGCACTGGATACGACAAAAATATG-3'; forward primer, 5'-GCGCGTCGTGAAGCGTTG-3', and reverse primer, 5'-GTGCAGGGTCCGAGGT-3'. For the detection of STAT3 mRNA and PTEN mRNA expression, qPCR was performed using QuantiTect SYBR Green PCR Kit (Qiagen, Germany). Glyceraldehyde-3-phosphate dehydrogenase (GAPDH) was used to normalize STAT3 mRNA and PTEN mRNA expression levels. The forward and reverse primer sequences for STAT3 mRNA were 5'-CTGTCAGATGCCAAATGC-3' and 5'-CTTACCCTGATGTCCTT-3', respectively. The forward and reverse primer sequences for PTEN mRNA were 5'-GAGGGATAAAACACCATG-3' and 5'-AGGGTAGGATGTGAACAGTA-3', respectively. The forward and reverse primer sequences for GAPDH were 5'-AACTTTGGCATTGTGGAAGG-3' and 5'-ACACATTGGGGGTAGGAAACA-3', respectively. All the experiments were performed in triplicate.

Western blotting analysis

Cells were washed, harvested, and prepared for Western blotting as previously described [36]. A total of 30 µg protein was separated using 8% sodium dodecyl sulfate polyacrylamide gel electrophoresis and transferred onto a nitrocellulose membrane. The membrane was incubated with the primary antibodies for STAT3, AKT and PTEN (1:1000), and then actin (1:5000) in 5% non-fat milk in Tris-buffered saline and Tween 20 at room temperature for 1 h, followed by exposure to a goat anti-rabbit or anti-mouse secondary antibody conjugated with horseradish peroxidase. Signals of the immunoreactive bands were visualized using the electrochemiluminescent detection system.

Transfection of anti-miR-21 into NPC cells

CNE1 and CNE2 cells was maintained in Dulbecco's Modified Eagle Medium, supplemented with 100 U/ml penicillin, 100 µg/ml streptomycin and 10% fetal bovine serum (Invitrogen, USA). For transfection, the anti-miR-21 or control, and miR-21 high expression plasmid or control (Exiqon A/S, Denmark) were delivered at a final concentration of 50 nM using Lipofectamine 2000 reagent (Life Technologies, USA).

Cell proliferation and colony formation assay

Cells were plated in 96-well plates (5000 cells/well), incubated for 48 h, and then transfected with 50 nM miR-21 mimics, its inhibitor or negative control. At the end of the incubation, cell proliferation reagent WST-8 (10 µl) was added to each well and incubated for 3 h at 37°C. Viable cell numbers were estimated by measuring optical density at 450 nm.

For the colony formation assay, 50 nM miR-21 mimics or its inhibitor was transfected into CNE1 cells, which were cultured in medium containing 10% fetal bovine serum, with the medium being refreshed every 3 days. After incubation for 14 days, cells were fixed with methanol and stained with 0.1% crystal violet (Sigma-Aldrich, USA). Visible colonies were manually counted. Triplicate wells were measured in each group.

Annexin V-fluorescein isothiocyanate (FITC)/propidium iodide (PI) double staining

The Annexin-V-FITC/PI double staining assay was used to detect cellular apoptosis. CNE1 and CNE2 cells were transfected with 50 nmol/l of miR-21 mimics or negative control. At the end of incubation, the cells were collected, washed with cold PBS and resuspended at 1×10^6 cells/ml in Annexin-V binding buffer. The supernatant (100 µl/tube) was incubated with 5 µl Annexin-V-FITC and 5 µl PI for 15 min at room temperature in the dark. Binding buffer (400 µl) was then added to each tube, followed by cytometric analysis within 1 h of staining. All experiments were repeated for three times.

Animals

Five- to six-week-old female BALB/c-nude mice (Shanghai Laboratory Animal Co., Ltd., China) were used for experimental tumorigenicity assays. To facilitate estrogen-dependent xenograft establishment, each mouse received 17-estradiol (20 mg/kg; Sigma-Aldrich, USA) intraperitoneally once a week. One week after the treatment, equivalent amount of CNE1 cells, treated with miR-21 or control (100 nM for 48 h; Panagene, Inc., Korea) without transfection reagents according to the manufacturer's protocol, were injected subcutaneously (10^7 cells/tumor) into the right axilla of nude mice [37]. The mice were weighed, and tumor width (W) and length (L) were measured every day. Tumor volume was estimated according to the standard formula $V = \pi/6 \times L \times W^2$,

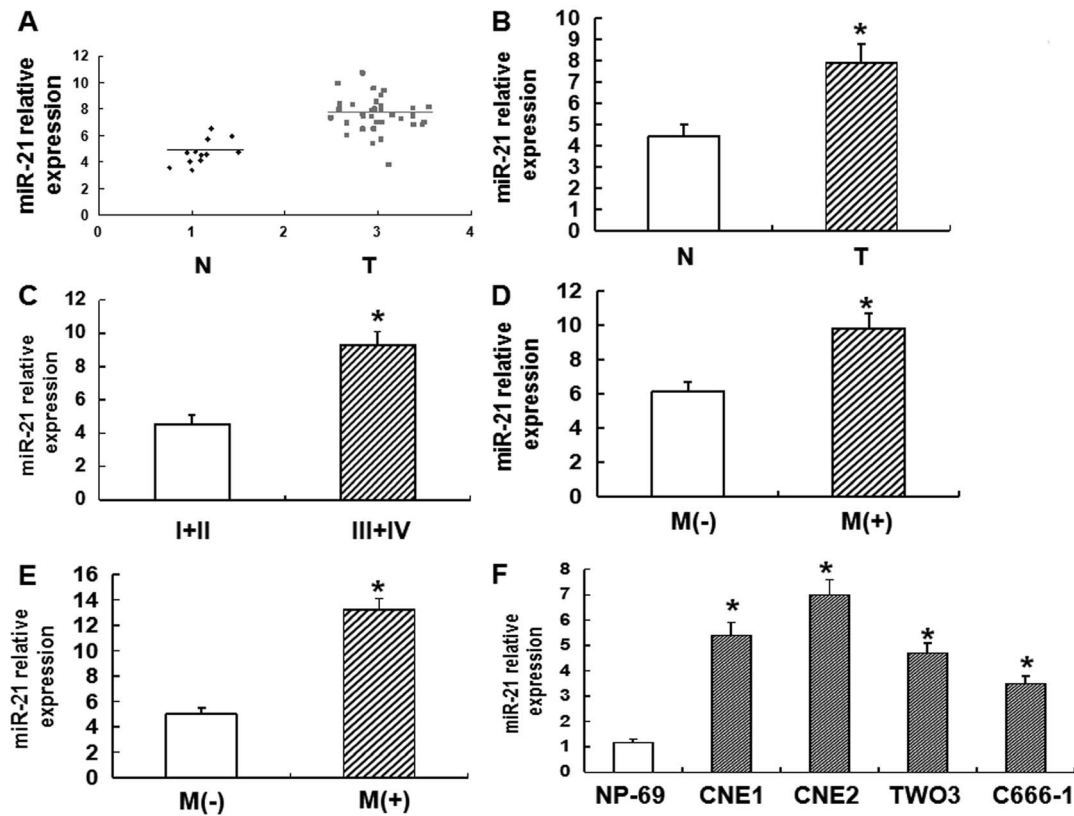


Figure 1. Expression of miR-21 in various tissues or cell lines. (A) Relative expression of miR-21 in non-tumor tissues ($n = 12$) and NPC tissues ($n = 42$). RT-PCR was used to determine the expression of miR-21, which was normalized to U6 expression to obtain relative expression. N, non-tumor tissues; T, tumor tissues. (B) Histograms of the average relative expression of miR-21 in non-tumor tissues ($n = 12$) and NPC tissues ($n = 42$). Data are means \pm SD. Asterisks indicate values that are significantly different from the values of non-tumor tissues ($P < 0.05$). (C) Histograms of the average relative expression of miR-21 in patients at stages I+II and III+IV. Data are means \pm SD. Asterisks indicate values that are significantly different from the values of patients at stage I+II ($P < 0.05$). (D) Histograms of the average relative expression of miR-21 in patients without and with distant metastasis. Data are means \pm SD. Asterisks indicate values that are significantly different from the values of patients without distant metastasis ($P < 0.05$). M, distant metastasis. (E) Histograms of the average relative expression of miR-21 in patients without and with lymph node metastasis. Data are means \pm SD. Asterisks indicate values that are significantly different from the values of patients without lymph node metastasis ($P < 0.05$). M, lymph node metastasis. (F) Histograms of the average relative expression of miR-21 in normal nasopharyngeal epithelial cell line (NP-69) and NPC cell lines (CNE1, CNE2, TWO3, and C666-1). Data are means \pm SD. Asterisks indicate values that are significantly different from the values of NP-69 ($P < 0.05$). doi:10.1371/journal.pone.0109929.g001

as described previously [38]. Animals were killed 9 days after the initial growth of the CNE1 xenografts was detectable, and the tumors were extracted. In all experiments, the ethics guidelines for investigations in conscious animals were followed, with approval from the Ethics Committee for Animal Research at The First Affiliated Hospital of Guangxi Medical University.

Terminal deoxynucleotidyl transferase dUTP nick end labeling (TUNEL)

Nude mice were euthanized and frozen sections were prepared as described above. TUNEL assay was performed according to the manufacturer's instructions. Sections were visualized under a fluorescent microscope (Nikon, USA).

Luciferase reporter assay

The 3'-UTR segments of PTEN mRNA containing miR-21 binding sites were amplified by PCR from human genomic DNA, inserted into the Xba1-site of pGL3 vector (Promega, USA), and named as pGL3-PTEN-wt. Using pGL3-PTEN-wt as a template, mutations were introduced into the predicted miR-21 binding sites

by QuikChange site-directed mutagenesis kit (Stratagene, USA), and named as pGL3-PTEN-mut. CNE1 cells were transfected in 24-well plates with wild-type or mutant reporter plasmid vector by Lipofectamine 2000, and the cells were transfected again with miR-21 inhibitor or negative control at 6 h after the second transfection. After 36 h, luciferase activity was measured using dual luciferase assay system (Promega, USA). The firefly luciferase activity of each sample was normalized to Renilla luciferase activity.

Statistical analyses

Spearman's rank correlation test was used for correlation analysis between predicted target gene protein levels and endogenous miR-21 levels measured previously by RT-PCR [39]. Pearson's Chi-Square tests were used to compare target gene expression levels to clinicopathological characteristics. Survival curves were estimated by the Kaplan-Meier method and log-rank test. All analyses were performed using SPSS 16.0 for Windows (SPSS Inc., USA). All tests were two-tailed, and $P < 0.05$ was considered statistically significant.

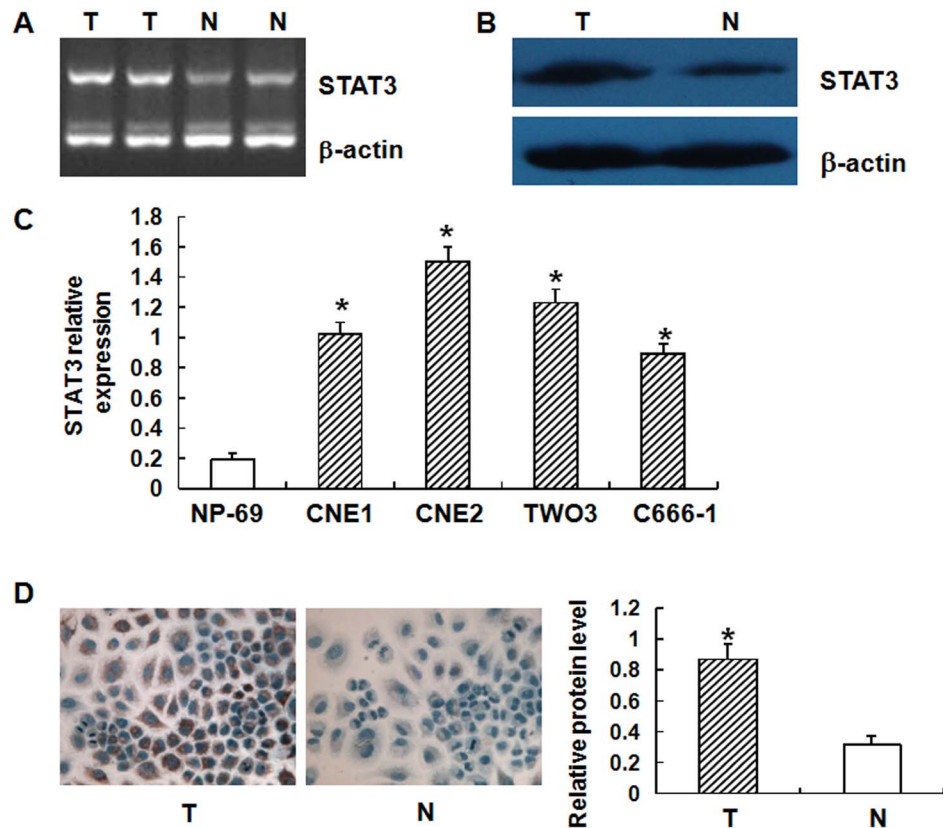


Figure 2. STAT3 expression in various tissues and cell lines. (A) Relative STAT3 mRNA levels in NPC tissues (T) and non-tumor tissues (N) determined by RT-PCR. The results were normalized to β -actin mRNA levels and were presented as relative STAT3 mRNA expression. Asterisks indicate values that are significantly different from the values of non-tumor tissues ($P < 0.01$). (B) Relative expression of STAT3 protein in NPC tissues (T) and non-tumor tissues (N) determined by Western blotting. STAT3 protein expression was normalized to β -actin protein expression. Asterisks indicate values that are significantly different from the values of non-tumor tissues ($P < 0.01$). (C) Relative expression of STAT3 mRNA in four NPC cell lines (CNE1, CNE2, TWO3, and C666-1) and normal nasopharyngeal epithelial cell line (NP-69) determined by RT-PCR. Asterisks indicate values that are significantly different from the values of NP-69 ($P < 0.01$). (D) Immunohistochemical staining and quantification of expression of STAT3 in NPC cell line CNE1 and normal nasopharyngeal epithelial cell line NP-69. The cytoplasm was counter-stained with hematoxylin. N, NP-69; T, CNE1. doi:10.1371/journal.pone.0109929.g002

Results

miR-21 is overexpressed in tissues and cell lines from NPC patients

To investigate the expression of miR-21, RT-PCR was employed. Our data showed that the expression of miR-21 in tissues from NPC patients was significantly higher than that in tissues from normal person ($P < 0.01$) (Fig. 1A and B). As the

advance of clinical tumor-node-metastasis stage (Fig. 1C), distant metastasis (Fig. 1D), and lymph node metastasis (Fig. 1E), the expression of miR-21 was enhanced. In addition, the expression of miR-21 in NPC cell lines CNE1, CNE2, TWO3, and C666-1 was elevated compared with that in normal nasopharyngeal epithelial cell line NP-69 ($P < 0.01$) (Fig. 1F). These data indicated that miR-21 was overexpressed in tissues and cell lines from NPC patients.

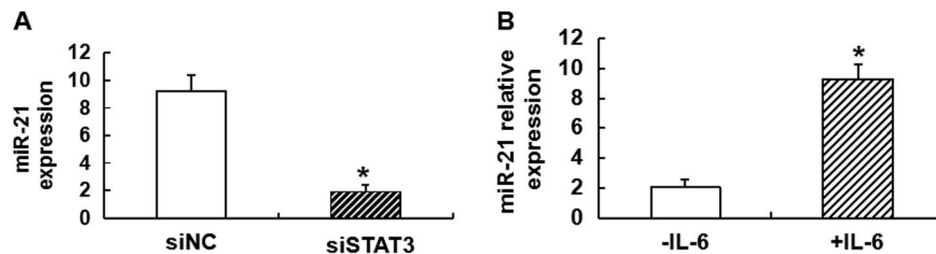


Figure 3. Expression of miR-21 regulated by STAT3 during transformation. (A) Levels of miR-21 expression in CNE1 cells after treatment with siSTAT3 and siNC. siSTAT3 indicates that STAT3 is inhibited by siRNA, while siNC indicates that STAT3 is not inhibited by siRNA. Data are means \pm SD. Asterisks indicate values that are significantly different from the values of siNC group. (B) Levels of miR-21 expression without (-IL-6) and with (+IL-6) IL-6 treatment of CNE1 cells. -IL-6 indicates that STAT3 is not activated by IL-6, while +IL-6 indicates that STAT3 is activated by IL-6. Data are means \pm SD. Asterisks indicate values that are significantly different from the group without IL-6 treatment. doi:10.1371/journal.pone.0109929.g003

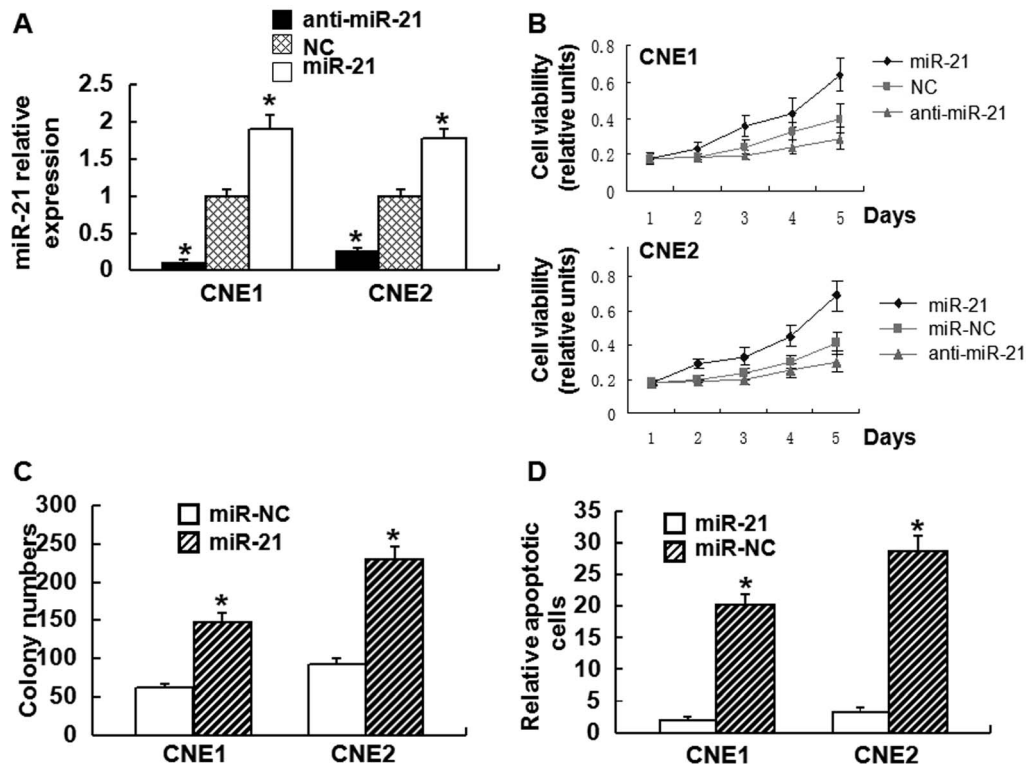


Figure 4. The effect of miR-21 on NPC cell growth and apoptosis *in vitro*. (A) Relative expression of miR-21 in CNE1 and CNE2 cells stably transfected by empty vector (NC) or vectors expressing miR-21 and anti-miR-21 detected by RT-PCR. The results were normalized to U6 expression and expressed as fold change relative to the corresponding negative control. anti-miR-21 is the inhibitor of miR-21. Data are means \pm SD. Asterisks indicate values that are significantly different from the NC group (n = 3). (B) Proliferation curve of CNE1 and CNE2 cells stably transfected by empty vector (NC) or vectors expressing miR-21 and anti-miR-21. Data are means \pm SD. Asterisks indicate values that are significantly different from the NC group (n = 3). (C) Representative results of colony formation of CNE1 and CNE2 cells transfected with miR-21 mimics and miR control (NC). Data are presented as means \pm SD. Asterisks indicate values that are significantly different from the NC group. (D) The apoptosis of CNE1 and CNE2 cells transfected with empty vector (NC) or vector expressing miR-21 detected by flow cytometry. Data are means \pm SD. Asterisks indicate values that are significantly different from the NC group. doi:10.1371/journal.pone.0109929.g004

STAT3 is up-regulated in NPC

To measure the expression of STAT3 mRNA and STAT3 protein, RT-PCR, Western blotting, and immunohistochemistry were used. The results showed that the levels of STAT3 mRNA and protein were significantly increased in NPC tissues compared with normal samples (Fig. 2A and B). In addition, the level of STAT3 mRNA was also enhanced in CNE1, CNE2, TWO3, and C666-1 cells compared with NP-69 cells (Fig. 2C). Immunohistochemical data also showed that STAT3 protein levels in CNE1 cells were higher than that in NP-69 cells. These data suggested that STAT3 was up-regulated in NPC.

STAT3 regulates the activity of miR-21 during transformation

To study how STAT3 regulates the activity of miR-21 during transformation, STAT3 binding to the targets sites in the miR-21 promoter was induced by interleukin (IL)-6 upon transformation, and the expression of miR-21 was measured by RT-PCR. The results showed that inhibition of STAT3 by siRNA strongly reduced miR-21 expression levels (Fig. 3A). By contrast, STAT3 activation by IL-6 in CNE1 cells resulted in up-regulation of miR-21 (Fig. 3B). These results strongly suggested that STAT3 function in transformation involved transcriptional activation of miR-21.

miR-21 stimulates NPC cell growth and inhibits apoptosis *in vitro*

To test the effect of miR-21 on the cell growth and apoptosis of NPC cells *in vitro*, transfection of CNE1 and CNE2 cell lines and flow cytometry were performed. After transfection, the miR-21 levels was increased by 90% in CNE1 cells, and 78% in CNE2 cells ($P < 0.01$), while knockdown of miR-21 by anti-miRNA reduced miR-21 levels by 88% in CNE1 cells, and 73% in CNE2 cells ($P < 0.01$) (Fig. 4A). miR-21 led to an increase in CNE1 and CNE2 cell growth and proliferation ($P < 0.05$, Fig. 4B and C). By contrast, anti-miR-21 decreased CNE1 and CNE2 cell growth ($P < 0.01$) (Fig. 4B). Flow cytometry data showed that overexpression of miR-21 significantly inhibited CNE1 and CNE2 apoptosis compared with the control ($P < 0.05$) (Fig. 4D). These data demonstrate miR-21 stimulated NPC cell growth and inhibited apoptosis *in vitro*.

miR-21 promotes tumor growth and suppresses apoptosis *in vivo*

To investigate the *in vivo* effect of miR-21, equal numbers (3×10^7) of CNE1 cells treated with miR-21 or the control were subcutaneously injected into nude mice (eight mice per treatment), and TUNEL and immunohistochemistry assays were performed. Detectable tumor masses (0.011 ± 0.014 g) were observed in all mice in the control group, while much larger tumors

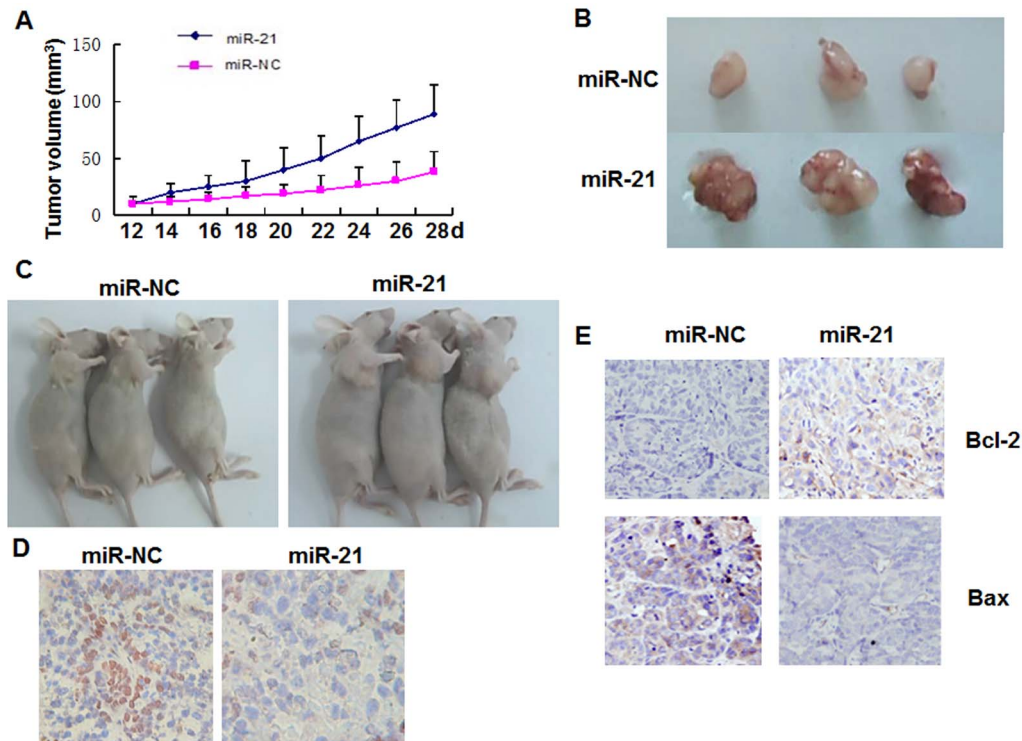


Figure 5. *In vivo* effect of miR-21 on CNE1 cell growth in nude mice. CNE1 cells (10^7 cells/tumor), treated with miR-21 or control (100 nM for 48 h) without transfection reagents, were injected subcutaneously into the right axilla of nude mice. **(A)** Growth curves for CNE1 cells treated with miR-21 ($n=8$) and control ($n=8$) obtained by *in vivo* proliferation assay. $P<0.05$ for all. **(B)** Photographs of tumors from miR-21 and control groups. **(C)** Photographs of mice from miR-21 and control groups. **(D)** Representative photomicrographs of CNE1 cells and apoptosis in miR-21 and control groups detected by TUNEL assay. **(E)** Representative photomicrographs of immunohistochemical staining and the relative levels of Bcl-2 and Bax on xenograft tumor sections obtained from mice in miR-21 and control groups. The cytoplasm was counter-stained with hematoxylin ($\times 400$). doi:10.1371/journal.pone.0109929.g005

(0.056 ± 0.032 g) were seen in all mice in the miR-21 group ($P<0.05$) (Fig. 5B and C). Data of tumor volume showed that CNE1 cells treated with miR-21 led to larger tumors more rapidly (Fig. 5A) than CNE1 control cells in nude mice. In addition, TUNEL assay data showed that fewer cells were undergoing DNA fragmentation after miR-21 treatment in mice (Fig. 5D). Cell survival in the early phase of apoptotic cascade depends mostly on the balance between pro-apoptotic and anti-apoptotic proteins of the Bcl-2 family. Bcl-2 family consists of anti-apoptotic factors such as Bcl-2 and pro-apoptotic factors such as Bax. In this study, we tested whether Bcl-2 and Bax protein levels were affected by miR-21. Furthermore, the expression of BCL-2 protein was significantly up-regulated, and the expression of BAX protein was dramatically down-regulated in the miR-21 treatment group compared with the control group (Fig. 5E). These results demonstrated that miR-21 promoted tumor growth and suppressed apoptosis *in vivo*.

miR-21 targets the PTEN tumor suppressor gene that functions through the Akt pathway

To measure the expression levels of miR-21 and PTEN mRNA in tissues and to validate whether miR-21 directly recognizes the 3'-UTRs of PTEN mRNA, we cloned a sequence with the predicted target sites of miR-21 or a mutated sequence with the predicted target sites to downstream of the pGL3 luciferase reporter gene and employed Western blotting assay. Statistical analysis showed that significant inverse correlation was observed between the levels of miR-21 and PTEN protein (Fig. 6A). In addition, inhibition of miR-21 expression results in up-regulation of PTEN mRNA expression (Fig. 6C and D). Similarly, inhibition

of miR-21 expression decreased the levels of phosphorylated AKT (Fig. 6C and D). When wild-type (wt) or mutant vector was transfected with miR-21, the luciferase activity of wt vector was significantly decreased ($P<0.001$) compared with mutant vector (Fig. 6B). By contrast, there was no significant difference between wt and mutant vector when transfected with negative control miRNA. These data suggested that miR-21 regulated PTEN expression at the post-transcriptional level and influenced the phosphorylation of AKT.

Discussion

In this study, we showed that miR-21 and STAT3 were elevated in the tissues and cell lines of NPC. Up-regulation of STAT3 is responsible for the activation of miR-21 during cellular transformation. In addition, we demonstrated that miR-21 promoted proliferation and suppressed apoptosis in NPC cell lines *in vitro* and *in vivo*. Finally, we showed that PTEN expression, as well as Akt phosphorylation, was regulated by miR-21 in NPC cell lines.

miR-21 was recently recognized as one of the most important biomarkers implicated in human malignancy. The up-regulation of miR-21 was observed in diverse types of malignancies such as lung cancer [10], [40–43], breast cancer [11], [44], gastrointestinal cancer [45–46], hepatocellular cancer [12], [47], prostate cancer [48]–[49], pancreatic cancer [50] bladder cancer [51], esophageal cancer [14], [52], NK-cell lymphoma [53], laryngeal carcinoma [54], and tongue squamous cell carcinomas [55]. In some types of cancers, high levels of miR-21 expression were linked to poor prognosis [10], [55–58]. However, it was not clear whether miR-

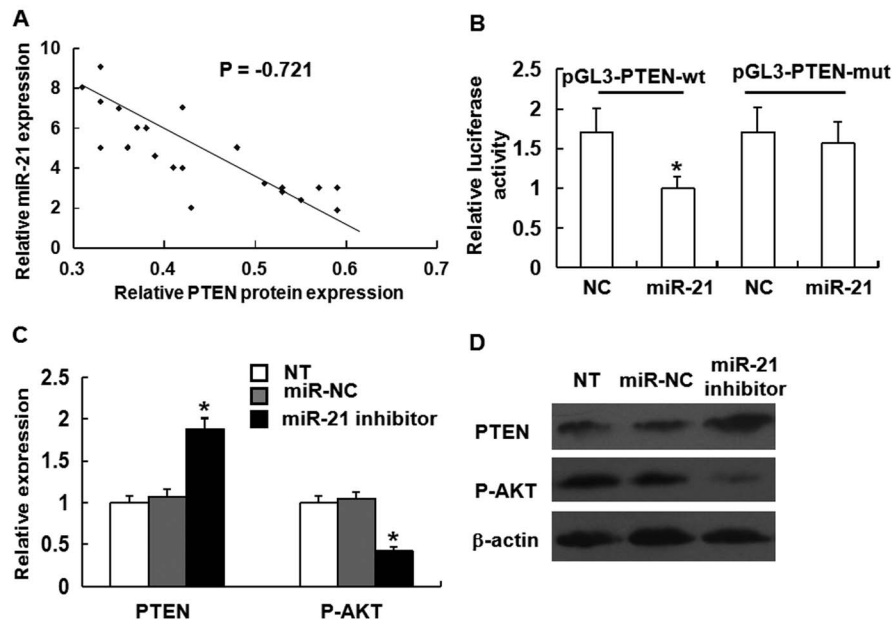


Figure 6. miR-21 regulates PTEN expression at the post-transcriptional level and influences the phosphorylation of AKT. Cells were transfected with miR-21 inhibitor, inhibitor-negative control (NC) or blank control culture medium (NT). Cell lysates were obtained after 48h for analysis. **(A)** Correlation between miR-21 expression and PTEN protein levels in NPC tissues (Pearson correlation = -0.721). **(B)** Relative luciferase activity of wt or mutant reporter plasmid co-transfected into CNE1 cells with miR-21 or negative control (NC). Luciferase activity was normalized to that of the control group to obtain relative luciferase activity. pGL3-PTEN-wt represents pGL3-PTEN wild-type plasmid vector, and pGL3-PTEN-mut represents pGL3-PTEN mutant reporter plasmid vector. Data were means \pm SD ($n=3$). Asterisks indicate values that are significantly different from the NC group ($P<0.01$). **(C)** Expression of PTEN and phosphorylated AKT examined by Western blotting. The results were normalized to β -actin protein expression and expressed as fold change relative to the corresponding negative control. Data were means \pm SD ($n=3$). Asterisks indicate values that are significantly different from the NT group ($P<0.01$). **(D)** Representative immunoblots of PTEN protein expression and the levels of phosphorylated AKT after treatment with negative control and miR-21 inhibitor. doi:10.1371/journal.pone.0109929.g006

miR-21 expression was changed in NPC. In the present study, we showed that miR-21 expression was significantly higher in NPC tissues and cell lines. Further, the up-regulation of miR-21 was observed in 29 out of 42 NPC tissues compared with non-tumor tissues. Specifically, 14 out of 22 NPC patients at stage III–IV showed miR-21 overexpression, while 15 out of 20 NPC patients with low miR-21 expression presented stage I–II disease. This study also showed miR-21 overexpression in 18 out of 24 NPC patients with lymph node metastasis, and 4 out of 5 patients with distant metastasis. Therefore, up-regulation of miR-21 occurred in NPC, and was associated with the stage of the disease. In CNE1, CNE2, TWO3, and C666-1 cells, the up-regulation of miR-21 was further confirmed by RT-PCR to play an important role in cell transformation. Thus, miR-21 was up-regulated in NPC, and associated with the clinical stage, as well as cancer metastasis.

The molecular mechanisms involved in the miR-21 regulation in cancer still remain unclear. Recent data showed that some transcription factors play an important role in miRNA expression. For example, p53/p63/p73 family binding sites modulate promoter activity of miRNAs of the miR-200 family, which are known regulators of cancer stem cells and epithelial-mesenchymal transitions [59]. STAT3-mediated overexpression of miR-17 blocked BIM protein expression and caused resistance to AZD6244 [60]. Activation of IL-6-STAT3 signaling caused the up-regulation of miR-23a expression in hepatocellular carcinoma [61]. These data suggested that transcription factors and miRNAs are associated with human cancers. In fact, in non-cancer cells, we previously described an intronic miRNA that suppresses the proliferation of vascular endothelial cells via the inhibition of STAT3 signaling [62]. In this study, we provided strong evidence

that the activation of miR-21 induced by STAT3 is important for cellular transformation. We found that STAT3 directly binds three sites in miR-21 promoter regions and is required for transcriptional induction of these miRNAs. On the other hand, inhibition of STAT3 by siRNA strongly reduced miR-21 expression levels. Conversely, STAT3 activation by IL-6 treatment in CNE1 cells resulted in the up-regulation of miR-21, suggesting that STAT3 and miR-21 are required for cellular transformation. This study further confirmed that STAT3 acts as a key molecule in the regulation of miRNA in cellular events and human diseases.

PTEN gene was first discovered and identified as a tumor suppressor gene [63], [64]. It was well known that PTEN induces apoptosis [65], [66] and controls cell growth [67] and angiogenesis [68] through interfering several signaling pathways. The key target of PTEN is phosphatidylinositol 3, 4, 5-trisphosphate [69]. PTEN is one of the most frequently inactivated tumor suppressors in different tumor types. Several mechanisms such as genetic mutation, promoter methylation, and post-transcriptional modification, may contribute to PTEN inactivation. In this study, it was found that PTEN expression was significantly down-regulated in NPC. PTEN expression was significantly increased, while the levels of phosphorylated Akt were decreased by miR-21 inhibitor. These findings suggest that the main mechanism of the reduction of PTEN protein is miRNAs regulation at post-transcriptional level. Recently, PTEN was reported as a direct target of miR-21 that was involved in miR-21-mediated effects on tumor biology: cell growth, migration, and invasion in human hepatocellular carcinoma [12] as well as gemcitabine-induced apoptosis in human cholangio carcinoma [69]. In this study, we observed a significant negative correlation between miR-21 and PTEN

protein in NPC. We postulated that miR-21 played an important role in the regulation of cell growth and apoptosis in NPC.

This postulation was verified by our experimental studies on NPC cell lines. miR-21 expression was increased in CNE1 and CNE2 cell lines, and cell growth was significantly increased in these cells transfected with miR-21. Meanwhile, cell apoptosis was significantly decreased by transfection of these cells with miR-21. These alterations concur with the observation in cancer tissues that the pro- and anti-apoptotic genes were changed. As discussed above, PTEN-AKT pathway was associated with miR-21 expression. It is reasonable to speculate that miR-21 promotes cell growth and/or inhibits apoptosis that is linked to PTEN expression. Given that PTEN inhibits tumor cell growth and invasion by blocking the PI3K/AKT pathway [70], we reached a

conclusion that miR-21 induces proliferation and inhibits apoptosis in NPC by targeting PTEN-AKT pathway.

In summary, miR-21 is overexpressed in NPC tissues, and promotes cell growth and suppresses apoptosis in NPC cell lines. These effects are linked to direct suppression of PTEN by miR-21. Our data suggested that miR-21 is a potential therapeutic target for NPC.

Author Contributions

Conceived and designed the experiments: MK. Performed the experiments: HO YL MK. Analyzed the data: HO YL MK. Contributed reagents/materials/analysis tools: HO YL MK. Wrote the paper: HO MK.

References

- Jeannel D, Bouvier G, Huber A (1999) Nasopharyngeal carcinoma: an epidemiological approach to carcinogenesis. *Cancer Surv* 33:125–155.
- Parkin DM, Bray F, Ferlay J, Pisani P (2002) Global cancer statistics. *CA Cancer J Clin* 55: 74–108.
- Yuan JM, Wang XL, Xiang YB, Gao YT, Ross RK, et al. (2000) Preserved foods in relation to risk of nasopharyngeal carcinoma in Shanghai, China. *Int J Cancer* 85: 358–363.
- Liebowitz D (1994) Nasopharyngeal carcinoma: the Epstein-Barr virus association. *Semin Oncol* 21: 376–381.
- Lo KW, Huang DP (2002) Genetic and epigenetic changes in nasopharyngeal carcinoma. *Semin Cancer Biol* 12: 451–462.
- Ambros V (2003) MicroRNA pathways in flies and worms: growth, death, fat, stress, and timing. *Cell* 13: 673–676.
- Esquela-Kerscher A, Slack FJ (2006) Oncomirs - microRNAs with a role in cancer. *Nat Rev Cancer* 6: 259–269.
- Chan JA, Krichevsky AM, Kosik KS (2005) MicroRNA-21 is an antiapoptotic factor in human glioblastoma cells. *Cancer Res* 65: 6029–6033.
- Fulci V, Chiaretti S, Goldoni M, Azzalin G, Carucci N, et al. (2007) Quantitative technologies establish a novel microRNA profile of chronic lymphocytic leukemia. *Blood* 109: 4944–4951.
- Yanaihara N, Caplen N, Bowman E, Seike M, Kumamoto K, et al. (2006) Unique microRNA molecular profiles in lung cancer diagnosis and prognosis. *Cancer Cell* 9: 189–198.
- Iorio MV, Ferracin M, Liu CG, Veronese A, Spizzo R, et al. (2005) MicroRNA gene expression deregulation in human breast cancer. *Cancer Res* 65: 7065–7070.
- Meng F, Henson R, Wehbe-Janek H, Ghoshalkar, Jacob ST, et al. (2007) MicroRNA-21 regulates expression of the PTEN tumor suppressor gene in human hepatocellular cancer. *Gastroenterology* 133: 647–658.
- Papagiannakopoulos T, Shapiro A, Kosik KS (2008) MicroRNA-21 targets a network of key tumor-suppressive pathways in glioblastoma cells. *Cancer Res* 68: 8164–8172.
- Hiyoshi Y, Kamohara H, Karashima R, Sato N, Imamura Y, et al. (2009) MicroRNA-21 regulates the proliferation and invasion in esophageal squamous cell carcinoma. *Clin Cancer Res* 15:1915–1922.
- Frankel LB, Christoffersen NR, Jacobsen A, Lindow M, Krogh A, et al (2008) Programmed cell death 4 (PDCD4) is an important functional target of the microRNA miR-21 in breast cancer cells. *J Biol Chem* 283: 1026–1033.
- Si ML, Zhu S, Wu H, Lu Z, Wu F, et al. (2007) miR-21-mediated tumor growth. *Oncogene* 26: 2799–2803.
- Zhu S, Wu H, Wu F, Nie D, Sheng S, et al. (2008) MicroRNA-21 targets tumor suppressor genes in invasion and metastasis. *Cell Res* 18: 350–359.
- Demaria M, Misale S, Giorgi C, Miano V, Camporeale A, et al. (2012) STAT3 can serve as a hit in the process of malignant transformation of primary cells. *Cell Death Differ* 19: 1390–1397.
- Demaria M, Poli V (2012) Pro-malignant properties of STAT3 during chronic inflammation. *Oncotarget* 3: 359–360.
- Giraud AS, Menheniott TR, Judd LM (2012) Targeting STAT3 in gastric cancer. *Expert Opin Ther Targets* 16: 889–901.
- Shodeinde AL, Barton BE (2012) Potential use of STAT3 inhibitors in targeted prostate cancer therapy: future prospects. *Onco Targets Ther* 5: 119–125.
- Pensa S, Regis G, Boselli D, Novelli F, Poli V (2009) STAT1 and STAT3 in Tumorigenesis: Two Sides of the Same Coin? JAK-STAT Pathway in Disease 100.
- Ai T, Wang Z, Zhang M, Zhang L, Wang N, et al. (2012) Expression and prognostic relevance of STAT3 and cyclin D1 in non-small cell lung cancer. *Int J Biol Markers* 27: 132–138.
- Barré B, Avril S, Coqueret O (2003) Opposite regulation of myc and p21waf1 transcription by STAT3 proteins. *J Biol Chem* 278: 2990–2996.
- Ettl T, Stiegler C, Zeidler K, Agaimy A, Zenk J, et al. (2012) EGFR, HER2, survivin, and loss of pSTAT3 characterize high-grade malignancy in salivary gland cancer with impact on prognosis. *Hum Pathol* 43: 921–931.
- Qu C, Liang Z, Huang J, Zhao R, Su C, et al. (2012) MiR-205 determines the radioresistance of human nasopharyngeal carcinoma by directly targeting PTEN. *Cell Cycle* 11: 785–796.
- Kurose K, Zhou X-P, Araki T, Cannistra S, Maher E, et al. (2001) Frequent loss of PTEN expression is linked to elevated phosphorylated Akt levels, but not associated with p27 and cyclinD1 expression, in primary epithelial ovarian carcinomas. *Am J Pathol* 158: 2097–2106.
- Panigrahi AR, Pinder SE, Chan SY, Paish EC, Robertson JFR, et al. (2004) The role of PTEN and its signalling pathways, including AKT, in breast cancer; an assessment of relationships with other prognostic factors and with outcome. *J Pathol* 204: 93–100.
- Netto G, Epstein J (2010) Theranostic and prognostic biomarkers: genomic applications in urological malignancies. *Pathology* 42: 384–394.
- Azim H, Azim H, Escudier B (2010) Targeting mTOR in cancer: renal cell is just a beginning. *Target Oncol* 5: 269–280.
- Xu J, Deng X, Tang M, Li L, Xiao L, et al. (2013) Tyrosylprotein sulfotransferase-1 and tyrosine sulfation of chemokine receptor 4 are induced by Epstein-Barr virus encoded latent membrane protein 1 and associated with the metastatic potential of human nasopharyngeal carcinoma. *PLoS One* 8: e56114.
- Yan L, Kang M, Qin Z, Zhang W, Li Y, et al. (2013) An intronic miRNA regulates expression of the human endothelial nitric oxide synthase gene and proliferation of endothelial cells by a mechanism related to the transcription factor SP-1. *PLoS One* 8: e70658.
- Wang LH, Kim SH, Lee JH, Choi YL, Kim YC, et al. (2007) Inactivation of SMAD4 tumor suppressor gene during gastric carcinoma progression. *Clin Cancer Res* 13: 102–110.
- Chern CJ, Beutler E (1976) Biochemical and electrophoretic studies of erythrocyte pyridoxine kinase in white and black Americans. *Am J Hum Genet* 28: 9–17.
- Chen C, Ridzon DA, Broomer AJ, Zhou Z, Lee DH, et al. (2005) Real-time quantification of microRNAs by stem-loop RT-PCR. *Nucleic Acids Res* 33: e179.
- Ou H, Shen YH, Utama B, Wang J, Wang X, et al. (2005) Effect of nuclear actin on endothelial nitric oxide synthase expression. *Arterioscler Thromb Vasc Biol* 25: 2509–2514.
- Wu L, Li Z, Zhang Y, Zhang P, Zhu X, et al. (2008) Adenovirus-expressed human hyperplasia suppressor gene induces apoptosis in cancer cells. *Mol Cancer Ther* 7: 222–232.
- Melo SA, Ropero S, Moutinho C, Aaltonen LA, Yamamoto H, et al. (2009) A TARBP2 mutation in human cancer impairs microRNA processing and DICER1 function. *Nat Genet* 41: 365–370.
- Yan LX, Huang XF, Shao Q, Huang MY, Deng L, et al. (2008) MicroRNA miR-21 overexpression in human breast cancer is associated with advanced clinical stage, lymph node metastasis and patient poor prognosis. *RNA* 14: 2348–2360.
- Yang M, Shen H, Qiu C, Ni Y, Wang L, et al. (2013) High expression of miR-21 and miR-155 predicts recurrence and unfavourable survival in non-small cell lung cancer. *Eur J Cancer* 49: 604–615.
- Markou A, Tsaroucha EG, Kaklamanis L, Fotinou M, Georgoulas V, et al. (2008) Prognostic value of mature microRNA-21 and microRNA-205 overexpression in non-small cell lung cancer by quantitative real-time RT-PCR. *Clin Chem* 54: 1696–1704.
- Cho WC, Chow AS, Au JS (2009) Restoration of tumour suppressor hsa-miR-145 inhibits cancer cell growth in lung adenocarcinoma patients with epidermal growth factor receptor mutation. *Eur J Cancer* 45: 2197–2206.
- Seike M, Goto A, Okano T, Bowman ED, Schetter AJ, et al. (2009) MiR-21 is an EGFR-regulated anti-apoptotic factor in lung cancer in never-smokers. *Proc Natl Acad Sci USA* 106: 12085–12090.
- Teng Y, Manavalan TT, Hu C, Medjakovic S, Jungbauer A, et al. (2013) Endocrine Disruptors Fludioxonil and Fenhexamid Stimulate miR-21 Expression in Breast Cancer Cells. *Toxicol Sci* 2013; 131: 71–83.

45. Kanaan Z, Rai SN, Eichenberger MR, Roberts H, Keskey B, et al. (2012) Plasma miR-21: a potential diagnostic marker of colorectal cancer. *Ann Surg* 256: 544–551.
46. Wu CW, Ng SS, Dong YJ, Ng SC, Leung WW, et al. (2012) Detection of miR-92a and miR-21 in stool samples as potential screening biomarkers for colorectal cancer and polyps. *Gut* 61: 739–745.
47. Bihrer V, Waidmann O, Friedrich-Rust M, Forestier N, Susser S, et al. (2011) Serum microRNA-21 as marker for necroinflammation in hepatitis C patients with and without hepatocellular carcinoma. *PLoS One* 6: e26971.
48. Li T, Li RS, Li YH, Zhong S, Chen YY, et al. (2012) miR-21 as an independent biochemical recurrence predictor and potential therapeutic target for prostate cancer. *J Urol* 187: 1466–1472.
49. Yang CH, Yue J, Fan M, Pfeffer LM (2010) IFN induces miR-21 through a signal transducer and activator of transcription 3-dependent pathway as a suppressive negative feedback on IFN-induced apoptosis. *Cancer Res* 70: 8108–8116.
50. Moriyama T, Ohuchida K, Mizumoto K, Yu J, Sato N, et al. (2009) MicroRNA-21 modulates biological functions of pancreatic cancer cells including their proliferation, invasion, and chemoresistance. *Mol Cancer Ther* 8: 1067–1074.
51. Catto JW, Miah S, Owen HC, Bryant H, Myers K, et al. (2009) Distinct microRNA alterations characterize high- and low-grade bladder cancer. *Cancer Res* 69: 8472–8481.
52. Alder H, Taccioli C, Chen H, Jiang Y, Smalley KJ, et al. (2012) Dysregulation of miR-31 and miR-21 induced by zinc deficiency promotes esophageal cancer. *Carcinogenesis* 33: 1736–1744.
53. Yamanaka Y, Tagawa H, Takahashi N, Watanabe A, Guo YM, et al. (2009) Aberrant overexpression of microRNAs activate AKT signaling via down-regulation of tumor suppressors in natural killer-cell lymphoma/leukemia. *Blood* 114: 3265–3275.
54. Liu M, Wu H, Liu T, Li Y, Wang F, et al. (2009) Regulation of the cell cycle gene, BTG2, by miR-21 in human laryngeal carcinoma. *Cell Res* 19: 828–837.
55. Li J, Huang H, Sun L, Yang M, Pan C, et al. (2009) MiR-21 indicates poor prognosis in tongue squamous cell carcinomas as an apoptosis inhibitor. *Clin Cancer Res* 15: 3998–4008.
56. Zaman MS, Shahryari V, Deng G, Thamminana S, Saini S, et al. (2012) Up-regulation of microRNA-21 correlates with lower kidney cancer survival. *PLoS One* 7: e31060.
57. Gao W, Shen H, Liu L, Xu J, Xu J, et al. (2011) MiR-21 overexpression in human primary squamous cell lung carcinoma is associated with poor patient prognosis. *Cancer Res Clin Oncol* 137: 557–566.
58. Gao W, Yu Y, Cao H, Shen H, Li X, et al. (2010) Deregulated expression of miR-21, miR-143 and miR-181a in non small cell lung cancer is related to clinicopathologic characteristics or patient prognosis. *Biomed Pharmacother* 64: 399–408.
59. Knouf EC, Garg K, Arroyo JD, Correa Y, Sarkar D, et al. (2012) An integrative genomic approach identifies p73 and p63 as activators of miR-200 microRNA family transcription. *Nucleic Acids Res* 40: 499–510.
60. Dai B, Meng J, Peyton M, Girard L, Bornmann WG, et al. (2011) STAT3 mediates resistance to MEK inhibitor through microRNA miR-17. *Cancer Res* 71: 3658–3668.
61. Wang B, Hsu SH, Frankel W, Ghoshal K, Jacob ST (2012) Stat3-mediated activation of microRNA-23a suppresses gluconeogenesis in hepatocellular carcinoma by down-regulating glucose-6-phosphatase and peroxisome proliferator-activated receptor gamma, coactivator 1 alpha. *Hepatology* 56: 186–197.
62. Yan L, Hao H, Elton TS, Liu Z, Ou H (2011) Intronic microRNA suppresses endothelial nitric oxide synthase expression and endothelial cell proliferation via inhibition of stat3 signaling. *Mol Cell Biochem* 357: 9–19.
63. Li J, Yen C, Liaw D, Podsypanina K, Bose S, et al. (1997) PTEN, a putative protein tyrosine phosphatase gene mutated in human brain, breast, and prostate cancer. *Science* 275: 1943–1947.
64. Steck PA, Pershouse MA, Jasser SA, Yung WK, Lin H, et al. (1997) Identification of a candidate tumour suppressor gene, MMAC1, at chromosome 10q23.3 that is mutated in multiple advanced cancers. *Nat Genet* 15: 356–362.
65. Leslie NR, Bennett D, Lindsay YE, Stewart H, Gray A, et al. (2003) Redox regulation of PI 3-kinase signalling via inactivation of PTEN. *EMBO J* 22: 5501–5510.
66. Stewart AL, Mhashilkar AM, Yang XH, Ekmekcioglu S, Saito Y, et al. (2002) PI3K blockade by Ad-PTEN inhibits invasion and induces apoptosis in radial growth phase and metastatic melanoma cells. *Mol Med* 8: 451–461.
67. Castellino RC, Durden DL (2007) Mechanisms of disease: the PI3K-Akt-PTEN signaling node -an intercept point for the control of angiogenesis in brain tumors. *Nat Clin Pract Neurol* 3: 682–693.
68. Machama T, Dixon JE (1998) The tumor suppressor, PTEN/MMAC1, dephosphorylates the lipid second messenger, phosphatidylinositol 3, 4, 5-trisphosphate. *J Biol Chem* 273: 13375–13378.
69. Meng F, Henson R, Lang M, Wehbe H, Maheshwari S, et al. (2006) Involvement of human microRNA in growth and response to chemotherapy in human cholangiocarcinoma cell lines. *Gastroenterology* 130: 2113–2129.
70. Vogt PK, Gymnopoulos M, Hart JR (2009) PI 3-kinase and cancer: changing accents. *Curr Opin Genet Dev* 19: 12–17.